J. Biomechanics Vol. 18, No. 5, pp. 317–328, 1985.
Printed in Great Britain

0021-9290/85 $3.00 + .00

THE MECHANICAL BEHAVIOUR OF CANCELLOUS BONE

L. J. GIBSON

Department of Civil Engineering, Massachusetts Institute of Technology, Cambridge, MA 02139, U.S.A.

Abstract—Cancellous bone has a *cellular* structure: it is made up of a connected network of rods and plates. Because of this, its mechanical behaviour is similar to that of other cellular materials such as polymeric foams. A recent study on the mechanisms of deformation in such materials has led to an understanding of how their mechanical properties depend on their relative density, cell wall properties and cell geometry. In this paper, the results of this previous study are applied to cancellous bone in an attempt to further understand its mechanical behaviour. The results of the analysis agree reasonably well with experimental data available in the literature.

NOMENCLATURE

C_1–C_3	constants of proportionality (–)
E	Young's modulus of cancellous bone (GN m^{-2})
E_s	Young's modulus of the solid bone in the cell wall (GN m^{-2})
F	force (N)
I	second moment of area of cross-section (m^4)
l	length of trabeculae (m)
M_p	internal plastic moment in a member (Nm)
P_{cr}	critical Euler buckling load (N)
t	thickness of trabeculae (m)
δ	beam deflection (m)
ε	strain (–)
ρ	density of cancellous bone (kg m^{-3})
ρ_s	density of the solid bone in the cell wall (kg m^{-3})
ρ/ρ_s	relative density of cancellous bone (–)
σ	stress (MN m^{-2})
σ^*	compressive strength of cancellous bone (MN m^{-2})
σ^*_{el}	elastic collapse stress in a cellular material (MN m^{-2})
σ^*_{pl}	plastic collapse stress in a cellular material (MN m^{-2})
σ_{ys}	yield stress of the solid bone in the cell wall (MN m^{-2})

INTRODUCTION

Bone occurs in two forms: as a dense solid (*compact bone*) and as a porous network of connecting rods or plates (*cancellous bone*). The most obvious difference between these two types of bone is in their relative densities, or volume fractions of solids. Bone with a volume fraction of solids less than 70% is classified as cancellous, that over 70% compact. Most bones in the body have both types, the dense compact bone forming an outer shell surrounding a core of spongy cancellous bone. In this configuration the bone forms a sandwich structure similar to man-made sandwich structures of fibreglass faces separated by a foam core. Like a man-made sandwich structure, the mechanical behaviour of the bone sandwich depends on the properties of its components and their geometry. This study describes the behaviour of one of those components, cancellous bone.

Cancellous bone is a cellular material made up of a connected network of rods or plates. A network of rods produces open cells while one of plates gives closed cells. Its mechanical behaviour is typical of a cellular material. The stress–strain curve of such materials has three distinct regimes of behaviour. In the first regime, behaviour is linear elastic as the cell walls bend or compress axially. Eventually, at high enough loads, the cells begin to collapse by elastic buckling, plastic yielding or brittle fracture of the cell walls. This second phase of collapse progresses at a roughly constant load until the cell walls meet and touch. Once this happens the resistance to load increases, giving rise to a final increasingly steep portion of the stress–strain curve.

The mechanical behaviour of cellular materials can be described by analyzing the mechanisms by which the cells deform (Gibson *et al.*, 1981; Gibson *et al.*, 1982; Gibson and Ashby, 1982; Easterling *et al.*, 1982). The results of the analysis depend on three parameters: the type of structure the cells form (for example, open or closed cells); the volume fraction of solids, or relative density; and the properties of the cell wall material. This paper attempts to apply this type of analysis to cancellous bone. Its structure is examined and modelled, the cell wall properties are identified and the analysis relates its mechanical behavior to its relative density. The results of the analysis describe the available data for mechanical properties reasonably well.

STRUCTURE OF CANCELLOUS BONE

The most extensive microscopic studies of the network structure of cancellous bone are those of Whitehouse, Dyson and Jackson in which they present scanning electron micrographs of cancellous bone in the human vertebrae, rib, femoral head, and sternum (Dyson *et al.*, 1970; Whitehouse *et al.*, 1971 a,b; Whitehouse and Dyson, 1974; Whitehouse, 1975). Their micrographs show various aspects of the structure. At low relative densities the cells form an open network of rods (Fig. 1). As the relative density increases, more material accumulates in the cell wall and the structure transforms into a more closed network of plates (Fig. 2). Some of the plate-like elements have small openings in them (for the marrow spaces to interconnect) resulting in cells which are not completely closed.

But because the plate-like features dominate the structure they are best modelled, in terms of cellular materials, as closed celled: in the remainder of the paper such perforated, plate-like structures are described as closed celled. Some micrographs show an asymmetrical structure of rods or plates, while others show cells with roughly columnar structure (Fig. 3).

Bone grows in response to the loads applied to it. The *density* of bone in a particular location depends on the *magnitude* of the applied loads. Whitehouse and Dyson (1974), in their study of the human femur, have presented micrographs from various regions in the head of the femur along with a density contour map of the same femur head. Comparison of the micrograph structures with the density map shows that low density, open cell, rod-like structures develop in regions of low stress while higher density, closed cell, plate-like structures occur in regions of higher stress. Their measurements of both femora and vertebrae show that the relative density of open cell, rod-like structures is typically less than 0.13 while that of closed cell, plate-like structures is over 0.2. At intermediate relative densities the structure is a combination of rod- and plate-like elements.

The *symmetry* of the structure in cancellous bone depends upon the *direction* of the applied loads. If the stress pattern in cancellous bone is complex, then the structure of the network of trabeculae is also complex and highly *asymmetric*. But in bones where the loading is largely uniaxial, such as the vertebrae, the trabeculae often develop a *columnar* structure with cylindrical symmetry (Weaver and Chalmers, 1966; Whitehouse *et al.*, 1971a). The columns of bone are oriented in the vertical direction: this gives relatively high stiffness and strength in the direction of load with lower stiffness and strength in the transverse directions. Observation of micrographs shows that both asymmetric and columnar structures can develop open or closed cells. This gives four basic types of structure for cancellous bone: the asymmetric, open cell, rod-like structure; the asymmetric, closed cell, plate-like structure; the columnar, open cell, rod-like structure; and the columnar, closed cell, plate-like structure.

COMPRESSIVE BEHAVIOUR

The stress–strain curve of cancellous bone in compression is typical of that of a cellular solid (Fig. 4). There are three regimes of behaviour: an initial linear portion, a plateau of almost constant stress, and a final increasingly steep region. Each of these three regimes has a distinct mechanism of deformation associated with it which depends upon the structure of the cells. At small strains the behavior is linear elastic. In cells with asymmetric structure, the rods or plates intersect at each other's mid-points, causing elastic bending of the cell walls (Pugh *et al.*, 1973). In cells with columnar structure, the rods or plates stack one on top of the other, and deformation in the longitudinal direction is by axial compression of the cell walls (Williams and Lewis, 1982). In the transverse direction, the cells do not align, and deformation is by bending the same as for asymmetric cells. At sufficiently high strains, the

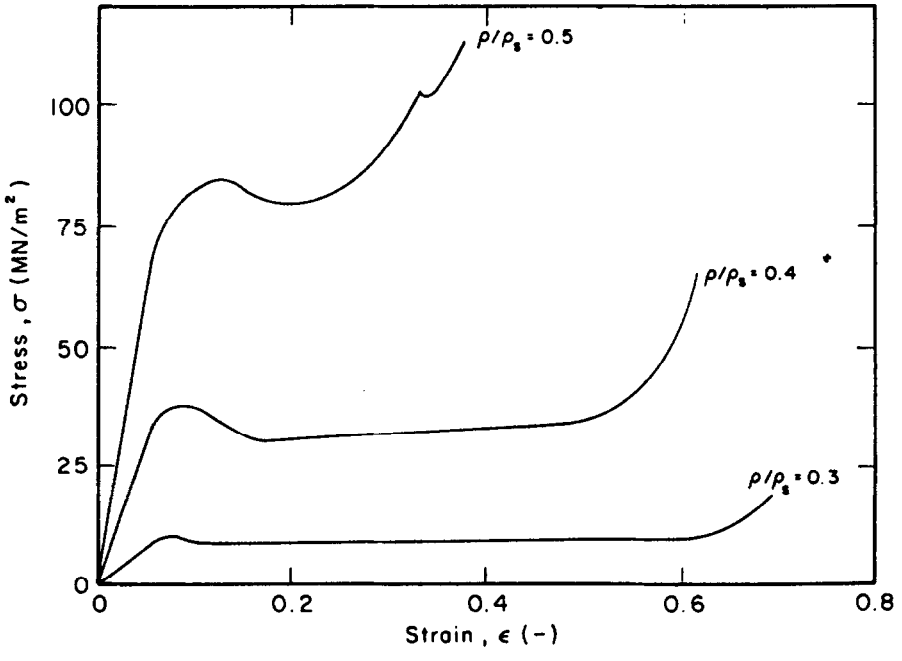

Fig. 4. Stress–strain curves for cancellous bone. As relative density increases, Young's modulus and compressive strength increase. The strain at which the cell walls touch and densification occurs decreases. (After Hayes and Carter, 1976.)

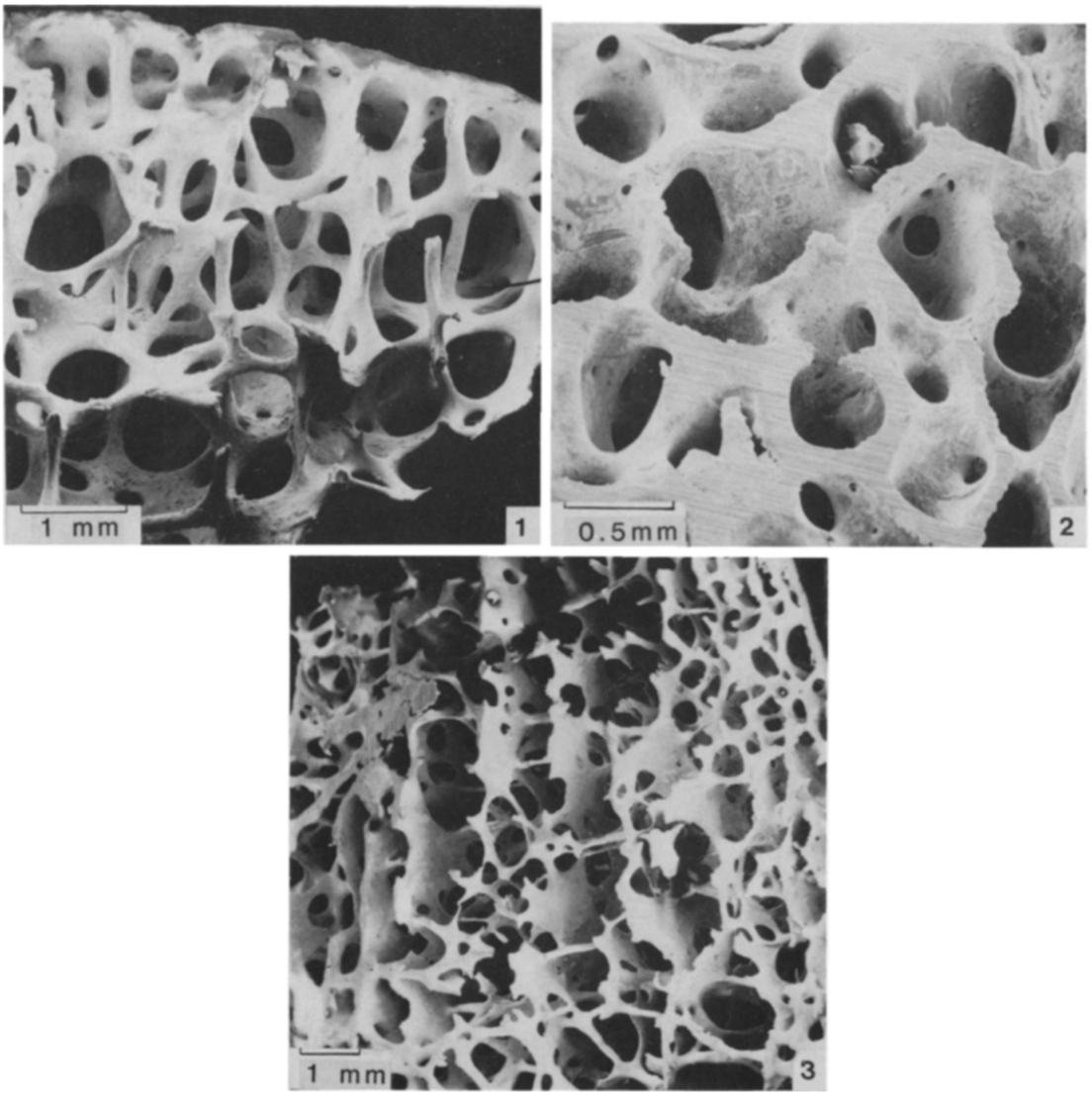

Fig. 1. Scanning electron micrograph of low density cancellous bone with an asymmetric rod-like structure. Specimen taken from the femoral head.

Fig. 2. Scanning electron micrograph of high density cancellous bone with an asymmetric plate-like structure. Specimen taken from the femoral head.

Fig. 3. Scanning electron micrograph of plate-like cancellous bone with columnar structure. Specimen taken from the femoral condyle.

cell fails by elastic buckling, by plastic yield, or by brittle fracture. If the rod or plate elements have a high ratio of length to thickness (slenderness ratio) failure is by elastic buckling, both in wet and dry specimens. But at lower slenderness ratios, wet specimens yield plastically while dry ones fracture in a brittle manner (Townsend *et al.*, 1975). Each of these failure mechanisms can occur in both asymmetric and columnar types of bone. Failure progresses at a roughly constant load until the cells close up sufficiently for the cell walls to touch. Once this happens the resistance to load increases giving rise to the final steeply rising portion of the stress–strain curve. As the density of cancellous bone increases the cell walls become thicker and the Young's modulus and compressive strength increase. The strain at which the cell walls touch decreases, reducing the length of the collapse stress plateau.

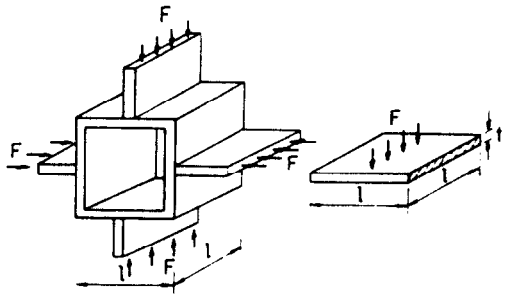

Fig. 6. Cubic model of plate-like asymmetric structure of cancellous bone. Square plates have side length, l, and thickness, t.

MODEL FOR CANCELLOUS BONE

The mechanical behavior of cellular materials can be modelled by idealizing the observed structures, characterizing the cell wall properties, and analyzing the mechanisms by which the cells deform. In the remainder of this paper the mechanical behaviour of cancellous bone will be modelled in this way.

Idealization of bone structures

Cancellous bone occurs in four configurations: as an asymmetric network of rods forming open cells; as an asymmetric network of plates forming closed cells; as a columnar network of rods forming open cells; and as a columnar network of plates forming closed cells. The models chosen for each of these structures must satisfy two requirements. The models must deform by the same mechanisms as the real structure, and they must be simple enough to analyze. The four models chosen are shown in Figs 5–8. The two cubic models relate to asymmetric open and closed cell structures and the hexagonal models relate to the open and closed cell columnar structures. The geometries chosen for the models are all simple and highly

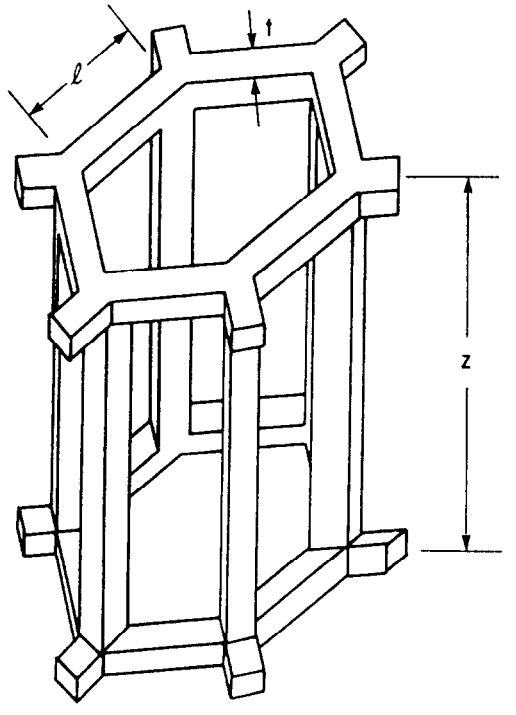

Fig. 7. Hexagonal model of rod-like columnar structure of cancellous bone. Hexagons have length, l, thickness, t, and depth, z.

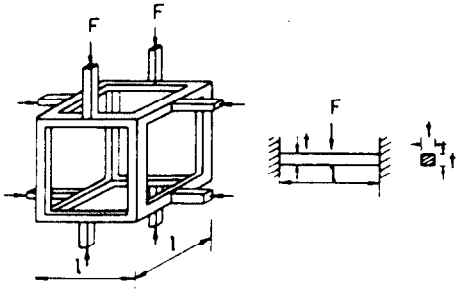

Fig. 5. Cubic model of rod-like asymmetric structure of cancellous bone. Struts have square cross-sections of side, t, and length, l.

idealized, and so geometric properties, such as anisotropy in asymmetric cancellous bone, are poorly modelled. The strength of the models lies in the fact that in each of the models the same mechanisms of deformation exist as in the actual structure. By using dimensional arguments, which do not depend on the exact geometry of the model selected but which are strongly dependent on reproducing the same mechanisms of deformation, the models can provide a useful basis from which to develop relationships between material properties and density.

Cell wall properties

In modelling cancellous bone the rod and plate elements, or trabeculae, are assumed to be made up of

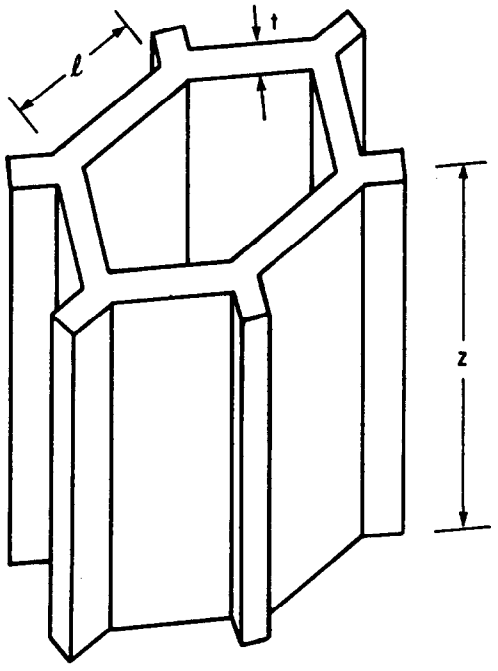

Fig. 8. Hexagonal model of plate-like columnar structure of cancellous bone. Hexagons have length, l, thickness, t, and depth, z.

compact bone. This assumption has been made by others (Carter and Hayes, 1977), but does not appear to have ever been verified. The density of compact bone is about 1800 kg m^{-3} (Carter and Hayes, 1977). Galante *et al.* (1970) measured the density of the trabeculae in 63 specimens of cancellous bone and found it to vary between 1400 and 2000 kg m^{-3} with a mean value of 1820 kg m^{-3}. Knowing the density of cancellous bone, ρ, and that of the trabeculae (or solid cell wall) ρ_s, allows calculation of a relative density, ρ/ρ_s. This is equivalent to the volume fraction of solids in the cancellous bone.

A typical stress–strain curve for wet compact bone is shown in Fig. 9. At small strains, it is linearly elastic. At higher strains plastic yielding occurs, both in tension and compression if the specimen is wet. Drying bone decreases its strain to failure; complete drying results in the elimination of yielding and failure by brittle fracture. The Young's modulus and tensile, compressive and flexural strengths for compact bone have been measured by several authors: for reviews see Currey (1970), Reilly and Burstein (1974), or Carter and Spengler (1978). There is a wide variation in the measured mechanical properties: the reviews give values of Young's modulus varying from 4 to 25 GPa, of tensile strength from 80 to 150 MPa, of compressive

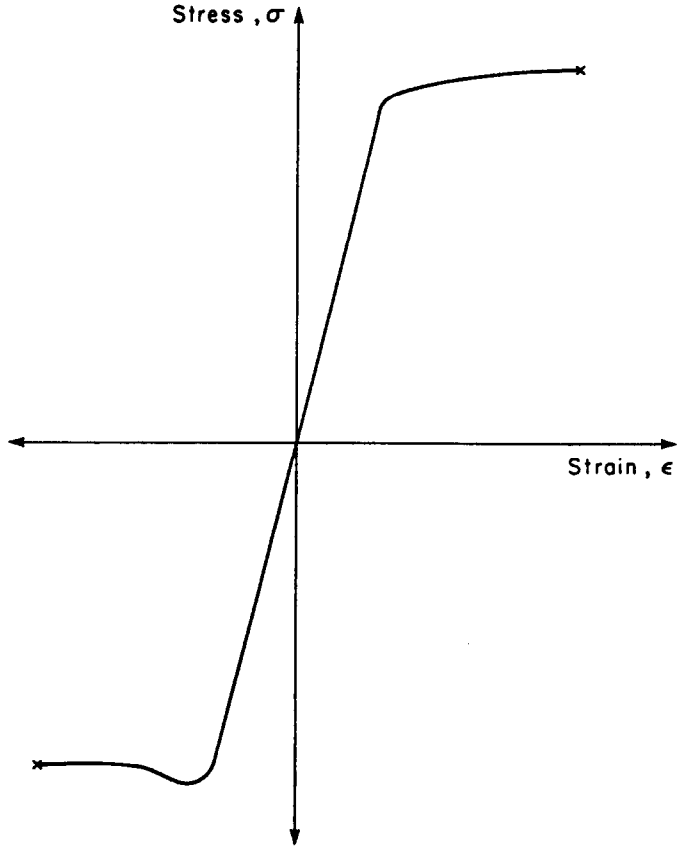

Fig. 9. Stress strain curve for wet compact bone (after Reilly and Burstein, 1974).

Table 1. Density dependence of properties of cellular materials

Property	Mechanism of deformation	Cubic open cell model†	Cubic closed cell model	Hexagonal model axial behaviour‡ Open cell	Closed cell
Relative density, ρ/ρ_s	—	$(t/l)^2$	(t/l)	$(t/l)^2$	(t/l)
Relative Young's Modulus, E/E_s	Cell wall bending	$(\rho/\rho_s)^2$	$(\rho/\rho_s)^3$	—	—
	Axial deformation	—	—	(ρ/ρ_s)	(ρ/ρ_s)
Elastic collapse stress, σ^*_{el}/E_s	Elastic buckling	$(\rho/\rho_s)^2$	$(\rho/\rho_s)^3$	$(\rho/\rho_s)^2$	$(\rho/\rho_s)^3$
Plastic collapse stress, $\sigma^*_{pl}/\sigma_{ys}$	Plastic yielding	$(\rho/\rho_s)^{3/2}$	$(\rho/\rho_s)^2$	(ρ/ρ_s)	(ρ/ρ_s)

ρ_s = density of solid cell wall material.
E_s = Young's Modulus of solid cell wall material.
σ_{ys} = yield strength of solid cell wall material.
†For derivation, see Gibson and Ashby (1982).
‡Transverse behaviour of hexagonal open and closed cell models is same as that for open and closed cell cubic models, respectively.

strength from 90 to 280 MPa, and of flexural strength from 150 to 240 MPa.

Analysis of mechanisms of deformation

Analysis of the cubic, closed cell model for the asymmetric, plate-like structure is presented here. Similar analyses for other structures have been reported elsewhere (Gibson and Ashby, 1982; Easterling *et al.*, 1982). The results of the analyses for all four structures are summarized in Table 1.

Consider the model of a cubic closed cell (Fig. 6). When a load, F, is applied, the cell walls initially deform by *bending*. If the cell wall material is linearly elastic, then the resulting deflection, δ, will be related to the applied load, F, by

$$\delta \propto \frac{Fl^3}{E_s I}$$

where E_s is the Young's modulus of the cell wall material and I is the second moment of area of the cross-section. For the closed cell plates, $I \propto lt^3$. The overall stress, σ, and strain, ε, are proportional to F/l^2 and δ/l respectively. Combining these results gives

$$E = \frac{\sigma}{\varepsilon} \propto E_s\left(\frac{t}{l}\right)^3.$$

Noting that for a closed cell, $\rho/\rho_s \propto t/l$

$$E/E_s = C_1(\rho/\rho_s)^3.$$

At higher loads the cells begin to collapse. The collapse may be caused by *elastic buckling*. If this occurs, the critical buckling load is given by the Euler equation

$$P_{cr} \propto \frac{E_s I}{l^2}.$$

Again the stress is proportional to P_{cr}/l^2 and the second moment of area of the cross-section, I, is proportional to lt^3. The resulting expression for the elastic collapse stress in the cell is

$$\sigma^*_{el} \propto E_s\left(\frac{t}{l}\right)^3$$

or

$$\sigma^*_{el}/E_s = C_2(\rho/\rho_s)^3.$$

If the cell wall can yield plastically then collapse may occur by a second mechanism. As the initial bending of the cell wall increases, yielding may occur, resulting in the formation of *plastic hinges*, and plastic collapse. Plastic hinges form when a cross-section has fully yielded. The internal plastic moment at which this occurs is given by

$$M_p \propto \sigma_{ys} t^2 l$$

where σ_{ys} is the yield stress of the solid cell wall material. The external moment applied to the section is proportional to the applied load, F, times the distance to the yielded cross-section, l. The internal and external moments must be equal for equilibrium, giving

$$M_p \propto \sigma_{ys} t^2 l \propto Fl.$$

Noting that the applied stress is proportional to F/l^2, then

$$\sigma^*_{pl} \propto \sigma_{ys}\left(\frac{t}{l}\right)^2$$

or

$$\sigma^*_{pl}/\sigma_{ys} = C_3(\rho/\rho_s)^2.$$

If the bone is dry, a third mechanism of failure exists: brittle fracture. Analysis of this mechanism has been described by Ashby (1983). As none of the data presented here are for dry bone, this analysis is not repeated.

The results for Young's modulus, and the elastic and plastic collapse stresses are presented in Table 1 along with the results of similar analyses for cubic open cell materials and columnar materials with cylindrical symmetry. Columnar cells deform by the same mechanisms as outlined above when loaded in the transverse direction. Their behaviour in axial compression is different. The cell walls do not bend but instead

contract axially: the modulus is then a direct function of the volume fraction of solids, or relative density. The strength of columnar cells in axial compression is governed by either elastic buckling or plastic yielding in the cell walls. The expression for the elastic buckling collapse stress is derived in the same manner as that for cubic cells. If yielding occurs, it is uniform over the cross section, and then the plastic collapse stress is linearly related to relative density.

EXPERIMENTAL RESULTS

Asymmetric cancellous bone has been investigated by several authors. Carter and Hayes (1977) report data for Young's modulus of cancellous bone from human tibia and bovine femoral condyles. The data are shown in Fig. 10. Compressive strength was investigated by Weaver and Chalmers (1966), Galante *et al.* (1970), Behrens *et al.* (1974), Hayes and Carter (1976) and Carter and Hayes (1977) (Fig. 11). Specimens in these tests were taken from the vertebrae, tibia, femur and calcaneus. Weaver and Chalmer's data for ash weights have been converted to density by dividing by 0.65. (Ash accounts for 65% of the weight of compact bone [Carter and Spengler, 1978].)

Williams and Lewis (1982) selected specimens with columnar structure from the proximal tibial epiphysis for their tests of Young's modulus and compressive strength. They tested specimens both in the axial and transverse directions and presented their results as a function of area fraction of bone. Their results are shown in Figs 12 and 13. All of the data in Figs 10-13 are for wet specimens.

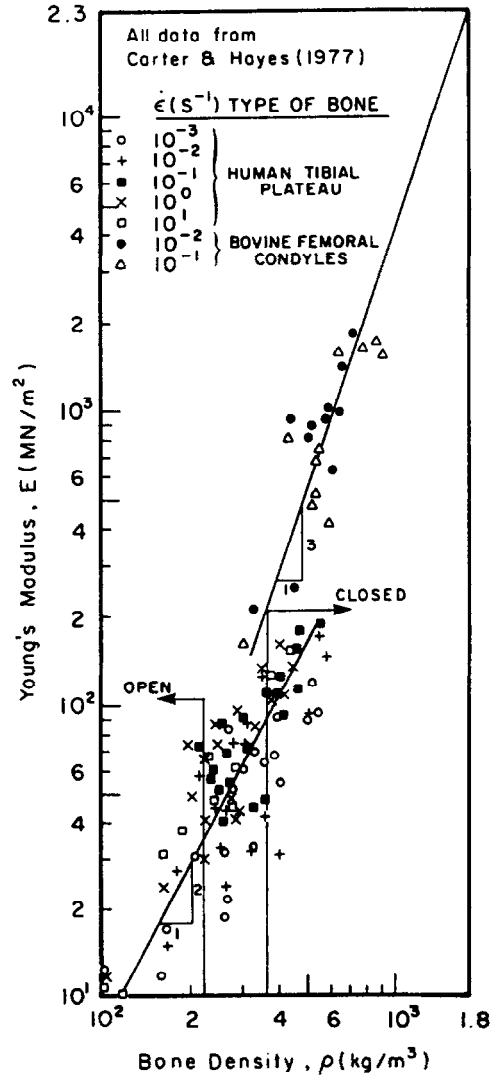

Fig. 10. Young's modulus plotted against density for cancellous bone with asymmetric structure.

DISCUSSION

Behaviour of asymmetric cancellous bone

Data for the Young's modulus of cancellous bone with an asymmetric structure are shown in Fig. 10. At densities less than about 350 kg m^{-3} the slope of the graph is 2, while at higher densities the slope is 3. Extrapolation of the higher slope gives Young's modulus for solid bone ($\rho = \rho_s = 1800$ kg m^{-3}) equal to 23 GPa. These test results are from confined uniaxial compression tests on cylindrical specimens. The use of a confining ring results in the data being higher than that which would be measured in an unconfined uniaxial test by a factor of about one-third. Reducing 23 GPa by this value gives an extrapolated value of Young's modulus for solid bone equal to 16 GPa, which is consistent with data for compact bone. The spread in the data is large: this is caused by two factors. The first is that there is some variability inherent in the Young's modulus of the cell wall bone as discussed earlier. The second is that the tests were carried out at strain rates varying over five orders of magnitude. Carter and Hayes (1977) report that Young's modulus varies with strain rate raised to the 0.06 power.

At low relative densities, the structure of cancellous bone is one of rods connecting to form open cells. This has been modelled as an open-celled cubic array of beam-like elements. At higher relative densities the cell walls fill in more, and the structure becomes one of the plates forming closed cells. This has been modelled as a closed cell cubic array of plate-like elements. The initial linear elastic behaviour of both of these structures occurs by bending of the cell walls. The analysis shows that Young's modulus should vary with the square of density for the open cell structure, and with the cube of density for the closed cell structure. This is exactly what the results of Carter and Hayes show. Their data suggest a transition from rod-like to plate-like elements at a density of about 350 kg m^{-3}, or relative density of 0.20. Micrographs from the Whitehouse study indicate the structure becomes fully plate-like at a relative density of 0.20, consistent with this.

Data for the compressive strength of cancellous bone with an asymmetric structure are shown in Fig. 11.

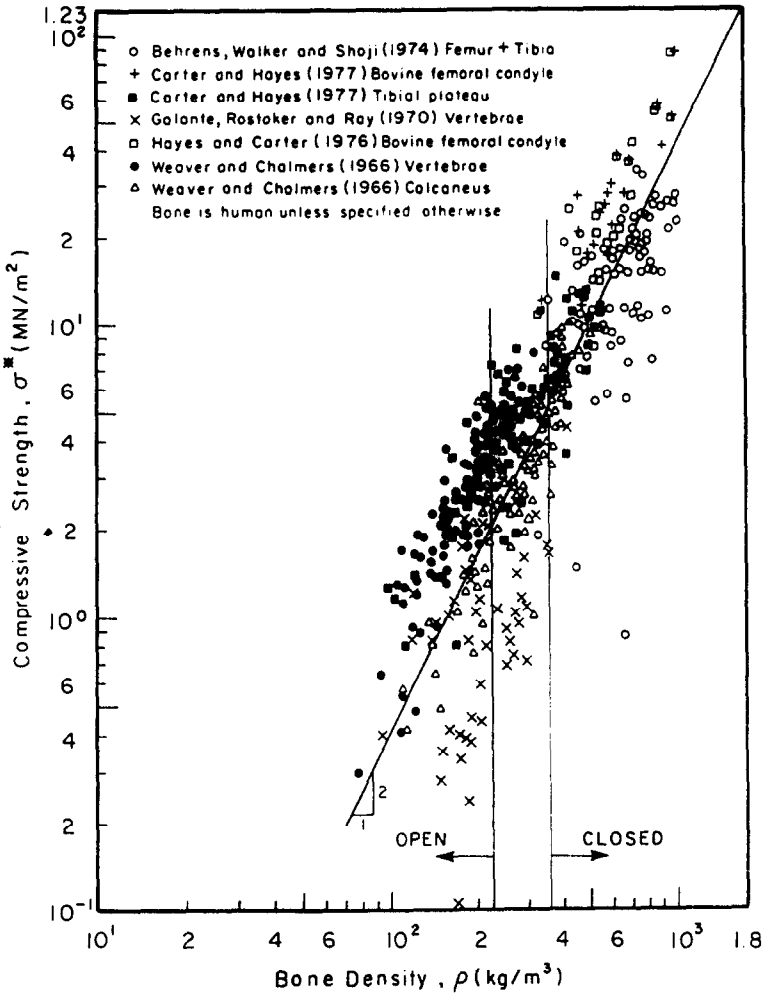

Fig. 11. Compressive strength plotted against density for cancellous bone with asymmetric structure.

The data fall on a line with a slope of 2 for all relative densities. Some sets of data are displaced slightly from the line drawn; these still have a slope of 2. This displacement and the resulting spread in the data, are again caused, to some extent, by the inherent variability in the cell wall properties. Extrapolation of the line drawn gives a compressive strength for solid bone of 123 MPa, consistent with reported values for compact bone.

Townsend *et al.* (1975) have tested single trabeculae in uniaxial compression. They found that slender, wet specimens (slenderness ratio, l/t, greater than 40) buckled elastically, while stockier ones yielded plastically. Dry specimens with a slenderness ratio greater than 10 buckled. Clearly then, cell wall collapse in cancellous bone may occur by either elastic buckling or the formation of plastic hinges in the bent cell walls. Which mechanism occurs depends on the slenderness ratio of the trabeculae, with elastic buckling occurring at the higher slenderness ratios or lower relative densities. As a result the data of Fig. 11 can be explained as follows. At low relative densities, the cells are open, and the trabeculae have a high slenderness ratio. They fail by elastic buckling and the resulting compressive collapse stress for open-celled asymmetric cancellous bone is related to the square of the density, as predicted from the analysis of the open cell model. At high relative densities, the cells are closed, and the trabeculae have lower slenderness ratios. They fail by plastic yielding and the resulting compressive collapse stress for asymmetric closed-cell cancellous bone is again related to the square of the density, as predicted from the analysis of the closed cell model. As a result, over the entire range of relative densities the compressive strength is related to the square of the density.

Behaviour of columnar cancellous bone

Williams and Lewis (1982) selected specimens with columnar structure for their tests. Data for the longitudinal and transverse Young's modulus of cancellous bone with a columnar structure are shown in Fig. 12. The data for the modulus in the longitudinal direction

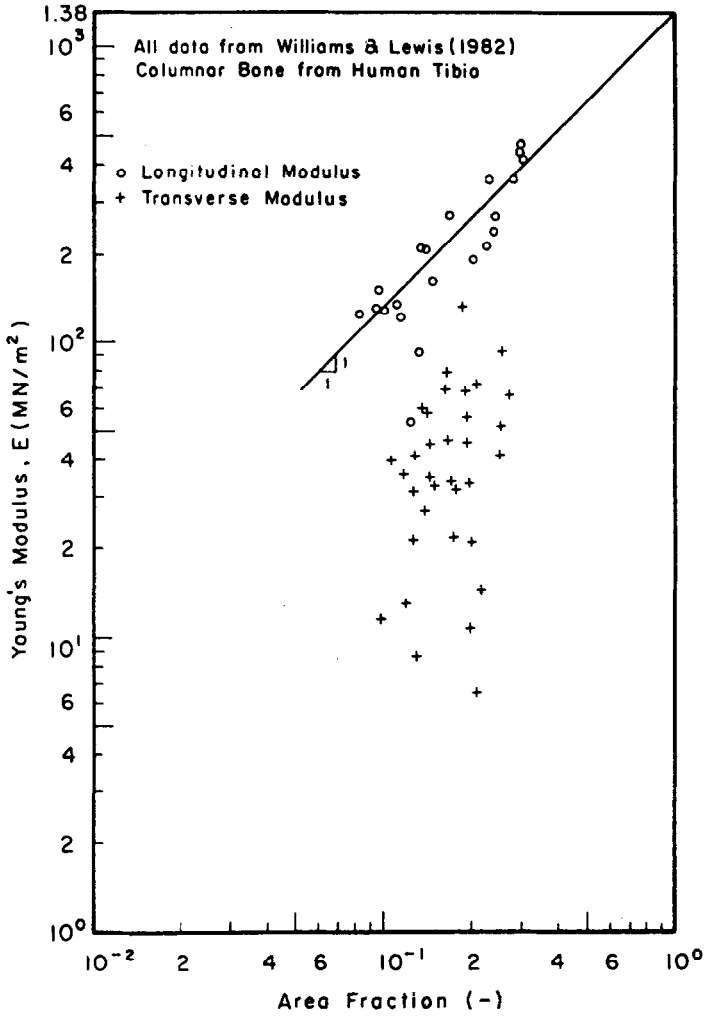

Fig. 12. Young's modulus plotted against area fraction for cancellous bone with columnar structure.

Table 2. Comparison of results of model with experimental data

Property	Relative density	Cell structure	Mechanism of deformation	Model prediction	Experimental Results
Asymmetric cells					
E	< 0.2	Open	Bending	ρ^2	ρ^2
	> 0.2	Closed	Bending	ρ^3	ρ^3
σ^*	< 0.2	Open	Elastic buckling	ρ^2	ρ^2
	> 0.2	Closed	Plastic yielding	ρ^2	ρ^2
Columnar cells					
E_{long}	All	Open and closed	Axial compression	ρ	ρ
E_{trans}	< 0.2	Open	Bending	ρ^2	—
	> 0.2	Closed	Bending	ρ^3	—
$\sigma^*_{pl\,long}$	All	Open and closed	Uniaxial plastic yielding	ρ	ρ
σ^*_{trans}	—	—	Elastic buckling or plastic yield	$\rho^{3/2}, \rho^2$ or ρ^3	—

fall on a line of slope of one, as is predicted by analyzing the axial compression of the cell walls. In the transverse direction, there is too much scatter in the data to develop any relationship between modulus and density. The model predicts a square dependence on density for open cells and a cubic density dependence for closed cells.

Williams and Lewis' data for the longitudinal and

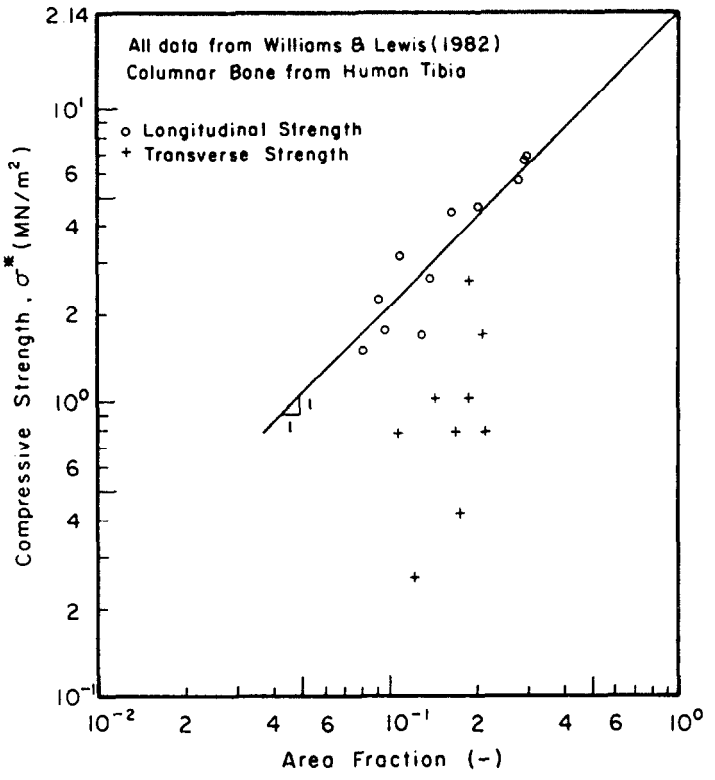

Fig. 13. Compressive strength plotted against area fraction for cancellous bone with columnar structure.

transverse compressive strength of columnar cancellous bone are shown in Fig. 13. Again the longitudinal strength appears to follow a line of slope 1: such a linear strength–density relationship is predicted by the model if failure is by plastic yielding. Again, in the transverse direction there is too much scatter in the data to develop any relationship between strength and density.

Table 2 summarizes the agreement between the models and experimental evidence. The mechanical behaviour of asymmetric cancellous bone is described well by the cubic model, both at low and high densities. The longitudinal behaviour of columnar cancellous bone can be explained in terms of the hexagonal model. More data on transverse stiffness and strength are required before the hexagonal model can be evaluated with respect to them.

CONCLUSIONS

Cancellous bone develops four types of structure. At low relative densities, it is made up of a network of rod-like elements which form open cells. At higher relative densities (greater than 0.2) it is made up of a network of plate-like elements forming closed cells. Under asymmetric loading conditions, the bone develops an asymmetric geometry. But when loading is largely uniaxial, as in some parts of the vertebrae for example, the structure can develop cylindrical symmetry. There are four resulting structures then: open and closed celled asymmetric, and open and closed celled columnar. Each of these structures can be modelled using an open or closed celled cubic or hexagonal array of beam or plate-like elements. Previous studies analyzing the mechanisms of deformation in such cellular materials have been used to derive relationships between material properties, such as stiffness and strength, and density. Data from several experimental studies on mechanical behaviour have been collated and plotted. The models for asymmetric structures (both open and closed celled) describe the experimental data well. The model for columnar cancellous bone explains the linear density dependence of longitudinal stiffness and strength. Additional experimental data is necessary to verify the columnar model in the transverse direction.

Acknowledgements—The author would like to thank Dr. D. Zielke for the loan of an article on osteoporosis which first stimulated her interest in this subject. Discussions of the project with Drs. D. Mofflin and W. Ovalle were most helpful and are greatly appreciated. Dr. K. Donelly generously provided bone specimens for the scanning electron microscopy and Mrs. M. Mager assisted in taking the micrographs. Mr. W. Janzen assisted in the preparation of Figs 9–12 and Mrs. K. Lamb typed the manuscript; their help is also gratefully acknowledged.

REFERENCES

Ashby, M. F. (1983) The mechanical behaviour of cellular solids. *Met. Trans.* **14A**, 1755–1769.
Behrens, J. C., Walker, P. S. and Shoji, H. (1974) Variations in

strength and structure of cancellous bone at the knee. *J. Biomechanics* **7**, 201–207.

Carter, D. R. and Hayes, W. C. (1977) The compressive behaviour of bone as a two-phase porous structure. *J. Bone Jt Surg.* **59A**, 954–962.

Carter, D. R. and Spengler, D. M. (1978) Mechanical properties and composition of cortical bone. *Clin. Orthop. Rel. Res.* **135**, 192–197.

Currey, J. D. (1970) The mechanical properties of bone. *Clin. Orthop. Rel. Res.* **73**, 210–231.

Currey, J. D. and Butler, G. (1975) The mechanical properties of bone tissue in children. *J. Bone Jt Surg.* **57A**, 810.

Dyson, E. D., Jackson, C. K. and Whitehouse, W. J. (1970) Scanning electron microscope studies of human trabecular bone. *Nature* **225**, 957–959.

Easterling, K. E., Harrysson, R., Gibson, L. J. and Ashby, M. F. (1982) On the mechanics of balsa and other woods. *Proc. R. Soc., London* **A383**, 31–41.

Galante, J., Rostoker, W. and Ray, R. D. (1970) Physical properties of trabecular bone. *Calcif. Tissue Res.* **5**, 236–246.

Gibson, L. J., Easterling, K. E. and Ashby, M. F. (1981). The structure and mechanics of cork. *Proc. R. Soc., London* **A377**, 99–117.

Gibson, L. J., Ashby, M. F., Schajer, G. S. and Robe. tson, C. I. (1982). The mechanics of two-dimensional cellular materials. *Proc. R. Soc., London* **A382**, 25–42.

Gibson, L. J. and Ashby, M. F. (1982) The mechanics of three-dimensional cellular materials. *Proc. R. Soc., London* **A382**, 43–59.

Hayes, W. C. and Carter, D. R. (1976) Postyield behaviour of subchondral trabecular bone. *J. biomed. Res. Symp.* **7**, 537–544.

Pugh, J. W., Rose, R. M. and Radin, E. L. (1973) A structural model for the mechanical behaviour of trabecular bone. *J. Biomechanics* **6**, 657–670.

Reilly, D. T., Burstein, A. H. and Frankel, V. H. (1974) The elastic modulus for bone. *J. Biomechanics* **7**, 271.

Reilly, D. T. and Burstein, A. H. (1974) The mechanical properties of cortical bone. *J. Bone Jt Surg.* **56A**, 1001.

Reilly, D. T., and Burstein, A. H. (1975) The elastic and ultimate properties of compact bone tissue. *J. Biomechanics* **8**, 393.

Townsend, P. R., Rose, R. M. and Radin, E. L. (1975) Buckling studies of single human trabeculae. *J. Biomechanics* **8**, 199–201.

Weaver, J. K. and Chalmers, J. (1966) Cancellous bone: its strength and changes with aging and an evaluation of some methods for measuring mineral content. I Age Changes in Cancellous Bone. *J. Bone Jt Surg.* **48A**, 289–298.

Whitehouse, W. J., Dyson, E. D. and Jackson, C. K. (1971a) The scanning electron microscope in studies of trabecular bone from the human vertebral body. *J. Anat.* **108**, 481–496.

Whitehouse, W. J., Dyson, E. D. and Jackson, C. K. (1971b) A fine structure in the trabeculation of the human rib. *Brit. J. Radiol.* **44**, 367–372.

Whitehouse, W. J. and Dyson, E. D. (1974) Scanning electron microscope studies of trabecular bone in the proximal end of the human femur. *J. Anat.* **118**, 417–444.

Whitehouse, W. J. (1975). Scanning electron micrographs of cancellous bone from the human sternum. *J. Pathol.* **116**, 213–224.

Williams, J. L. and Lewis, J. L. (1982) Properties and an anisotropic model of cancellous bone from the proximal tibial epiphysis. *J. biomech. Engng* **104**, 50–56.